

# Cholesterol crystallite nucleation in supersaturated model biles from a thermodynamic standpoint

Chen-Lun Liu<sup>a,\*</sup>, William I. Higuchi<sup>b</sup>

<sup>a</sup>*Institute of Biotechnology, National Dong-Hwa University, Shou-Feng, Hualien Hsien 974, Taiwan, ROC*

<sup>b</sup>*Department of Pharmaceutics and Pharmaceutical Chemistry, College of Pharmacy, University of Utah, Salt Lake City, UT 84112, USA*

Received 2 April 2001; received in revised form 1 February 2002; accepted 20 March 2002

## Abstract

A rapid, silicone polymer film uptake method was used to determine the cholesterol (Ch) thermodynamic activity ( $A_T$ ) in taurocholate (TC)–lecithin (L) and taurochenodeoxycholate (TCDC)–L model biles supersaturated with Ch. Also, time-dependent quasielastic light scattering (QLS) measurements and microscopic observations were made to determine the nature of particle species and the Ch nucleation times. In all cases in which Ch–L vesicles were present, a linear relationship between the logarithm of Ch nucleation times and Ch  $A_T$  was found. These findings support that Ch  $A_T$  is the appropriate parameter that represents the Ch nucleation tendency and that vesicles are catalytic sites in the Ch nucleation process. When  $\text{Ca}^{2+}$ , a nucleation promoter ion, was present in the supersaturated model biles, the increased values of Ch  $A_T$  quantitatively correlated with shorter Ch nucleation times. These latter findings further demonstrate that Ch  $A_T$  is the dominant factor in explaining the Ch nucleation tendencies in supersaturated model biles.

© 2002 Elsevier Science B.V. All rights reserved.

**Keywords:** Cholesterol thermodynamic activity; Catalytic site

## 1. Introduction

Early studies have demonstrated that patients with cholesterol (Ch) gallstones have bile supersaturated with Ch and this led to the early viewpoint that the presence of Ch in bile in excess of the micellar solubilization capacity would lead to the formation of Ch gallstones [1,2]. Previously, the Ch saturation index (CSI), i.e., the ratio of the Ch concentration in a bile sample relative to its saturation solubility in that sample, was used to compare biles of gallstone patients with those of healthy humans [3]. Later, it was found that the Ch supersaturated bile was not uncommon in healthy humans who did not develop Ch gallstones [2]. This apparent discrepancy followed by evidence for the presence of Ch carriers other than micelles, i.e., Ch–phospholipid vesicles, led to the view that these carriers may help stabilize bile, which would otherwise be unstable with respect to Ch precipitation on the basis of micellar Ch solubilization alone. Subsequently, other factors such as the hypomotility of the gallbladder have also been thought to be possible triggers for gallstone formation [4–7].

Holan et al. [8,9] introduced the concept of the Ch nucleation time in human bile. They defined the Ch nucleation time as the time required for the first appearance of Ch crystals in crystal-free bile. They showed that vesicles in healthy biles were stable for many days without Ch nucleation but, in patients with Ch gallstones, vesicles were found to aggregate and nucleation occurred in a few days. Their findings suggested that vesicle aggregation is an important process in the Ch nucleation and gallstone formation. Nevertheless, recent findings have indicated that Ch may nucleate in supersaturated bile without prior aggregation and fusion of vesicles [10–12]. Therefore, it is important to further investigate the role of vesicles and other factors in the Ch nucleation process.

From a thermodynamic standpoint, the driving force for Ch nucleation and precipitation in supersaturated bile should be the thermodynamic activity ( $A_T$ ) of Ch. Lee et al. [13,14] described a silicone polymer uptake method for determining Ch  $A_T$  as it pertains to Ch nucleation. This technique required equilibration of the silicone polymer with the bile solution for 12–24 h and is feasible for the measurement of Ch  $A_T$  of unsaturated biles. However, in the supersaturated bile, Halpern et al. [15,16] have shown that the Ch nucleation times could potentially be less than 12 h, especially in biles with a

\* Corresponding author. Fax: +886-3-8661959.

E-mail address: cliu@mail.ndhu.edu.tw (C.-L. Liu).

high bile salt (BS)/lecithin (L) molar ratio. Because nucleation and crystal growth on the surface of the polymer may compromise both the Ch concentration determinations in the model bile and the Ch  $A_T$  measurements, it was considered necessary to improve the silicone polymer uptake method of Lee et al. [13,14] to substantially reduce equilibration times. Since the transfer of Ch into the silicone polymer was not diffusion-controlled in the silicone polymer itself but was interface-controlled, changing the thickness of the silicone film alone did not result in the desired reduction of equilibration times. Jain et al. [17] attempted to overcome the interfacial barrier by making the silicone polymer surface positively charged. This modified method was confirmed to be both satisfactory and useful in reducing the equilibration times to less than 1 h.

The modified rapid uptake method for Ch  $A_T$  determination was recently developed [18] to examine the possible correlation between the  $A_T$  for Ch in Ch-supersaturated BS–L solutions and the Ch nucleation times determined by quasielastic light scattering (QLS) measurements and by microscopic observations as a function of time in these solutions. QLS measurements have also provided information on the nature of the particulate species in the Ch supersaturated BS–L systems, i.e., whether micelles, vesicles and/or Ch crystallites are present. This previous investigation was limited to relatively few example experiments, which basically established that the approach for examining the relationship between Ch supersaturation, as represented by Ch  $A_T$ , and the Ch nucleation time was highly promising. In addition, the limited experiments indicated (1) that there was likely a strong correlation between Ch  $A_T$  and Ch nucleation times and (2) that Ch-L vesicles were likely catalytic sites of Ch nucleation.

The purpose of the present study was to provide a quantitative examination of the relationship between Ch  $A_T$  and Ch nucleation times over a wide range of conditions. The studies were to include both taurocholate (TC)–L and the taurochenodeoxycholate (TCDC)–L systems. As will be seen, results of the present studies together with our previous results validate the role of vesicles and the importance of the Ch  $A_T$  interpretation in the Ch nucleation process.

## 2. Materials and methods

### 2.1. Materials

The thin silicone polymer film (Silastic sheeting No. 500-3) was acquired from Dow Corning Company, Midland, MI. Prior to use, the thin film was washed with boiling 95% ethanol for 15 s, followed by a thorough rinse with boiling deionized water for a few seconds. Tetradecyldimethyl [3-(trimethoxysilyl)-propyl] ammonium chloride (TDTOP) was obtained as a 50% methanol solution from Petrarch Chemical Company, Bristol, PA. Sodium TC and sodium TCDC were purchased from Calbiochem Corpora-

tion, San Diego, CA. Their purities (>96%) were checked by a thin layer chromatography (TLC) procedure [19]. Egg yolk lecithin was purchased from Lipid Products (Surrey, UK) and its purity was also checked by TLC [20]. Ch was acquired from Sigma Chemical Company (St. Louis, MO) and was purified by recrystallization from 95% ethanol three times before use. Radioactive Ch monohydrate (ChM) crystals were prepared as described previously [21]. Other chemicals were analytical grade and were used as received.

### 2.2. Pretreatment of the silicone polymer

The silicone polymer film was pretreated with a cationic polymer solution as described earlier [17] so as to incorporate a positive charge on the silicone polymer surface. The thin silicone polymer film ( $20 \times 1 \times 0.0254$  cm) was placed in a glass vial containing an aliquot of 0.6 ml 50% TDTOP diluted with 17.4 ml of methanol. The thin film was allowed to soak for 3 h with occasional shaking. At the end of 3 h, 2 ml of water was added to make the final TDTOP concentration equal to 1.5% and the thin film was left in this solution for another 12 h. Finally, the thin film was removed and dried overnight in a 37 °C incubator before cutting into  $2 \times 1 \times 0.0254$  cm sections and used in the uptake studies.

### 2.3. Ch $A_T$ measurement

Basically, the procedures in the present study are quite similar to those that have been published [17,18]. The BS–L–Ch admixtures were heated at 80 or 90 °C until isotropically clear and were filtered while still hot. The hot filtrate (1.5 ml) and a section of the pretreated thin film were added to each sample vial. The thin film was placed in an arched position to ensure its complete immersion in the solution. After flushing with nitrogen, the vials were tightly capped and were shaken on a rotating shaker maintained at 37 °C. At predetermined time intervals ( $\sim 1$  h), vials were successively removed and duplicate samples (100  $\mu$ l) of the model bile solution were taken and assayed for Ch concentration using a scintillation counter (Beckman Instruments, Irvine, CA). The thin polymer film was removed from the vial and quickly rinsed with three portions (10 ml each) of ethanol/water (1:4) mixture. The washed film was transferred to a scintillation vial and extracted for a minimum of three times with 3 ml portions of ethanol until no further radioactivity was observed in the final extract. The radioactivity from each extract was combined to determine the amount (and hence the concentration,  $C_{sp}$ ) of Ch partitioned in the silicone polymer. The Ch  $A_T$  value was determined ( $\pm 10\%$  error) based on the following equation [13,14,17,18,21,22]:

$$\text{Ch } A_T = C_{sp}/C_{sp}^{\circ} \quad (1)$$

where  $C_{sp}^{\circ}$  is the  $C_{sp}$  value at ChM saturation.

## 2.4. QLS measurement

Culture tubes (12 × 75 mm, American Scientific Products, McGaw Park, IL) were soaked in chromic acid overnight and then rinsed with distilled deionized water. The washed tubes were transferred into an 80 °C oven and dried. The procedure used in QLS sample preparation is similar to that described above for Ch  $A_T$  measurement except that after the clear solution was filtered at 80 °C, it was collected in the cleaned culture tubes and transferred into a 37 °C incubator without shaking.

The procedure used for QLS measurement is similar to that described earlier [27]. Briefly, the angle between the incident beam and the scattered beam was 90° to minimize stray light. A Cooper Laser Sonics (Model 95) argon ion laser operated at 514.5 nm wavelength and a temperature-controlled water bath maintained at 37 °C were part of the light-scattering apparatus. QLS measurements were performed with a Brookhaven BI-2030, extendable 72-channel, multi-bit correlator/computer. The scattered intensity from model bile solution was normalized by that from toluene ( $I_{\text{sol}}/I_{\text{tol}}$ ). By analyzing the random fluctuations in scattered intensity, the autocorrelation function, i.e., the repetitive comparisons of the intensity of scattered light from different channels was calculated [23,24]. The mean hydrodynamic radius ( $\bar{R}_h$ ) and polydispersity ( $V$ ) of the different species, i.e., micelles and vesicles, were determined as described previously [18,25–27]. Briefly, three particle populations could be identified as follows: (a) those with an  $\bar{R}_h$  value between 10 and 55 Å were categorized as micelles (including both simple and mixed micelles), (b) those with an  $\bar{R}_h$  value from 150 to 700 Å were classified as vesicles, and (c) those with an  $\bar{R}_h$  value >700 Å were characterized as aggregated vesicles, multilamellar vesicles or Ch crystallites.

## 2.5. Polarizing microscope nucleation time studies

Nucleation times (crystal observation times) were determined by experiments in which crystal (either needle or plate) appearance was observed microscopically. In general, several (5–10) 4-ml vials containing model bile solution at each supersaturation condition were maintained separately in an oven at 37 °C. They were successively removed at

predetermined time intervals (every 3 h for the first day and once a day for the remaining days) and the model bile solution examined with a polarizing microscope (Nikon, Garden City, NY). The sample was placed on a clean flat microscope slide covered with a coverglass and observed immediately. Photographs were taken in complete extinction under crossed Nicols.

## 3. Results and discussion

### 3.1. Correlation between Ch $A_T$ and Ch nucleation times

Previous studies [18] showed that nucleation of Ch crystallites in a supersaturated model bile may be catalyzed by Ch–L vesicles. In addition, QLS and microscopy studies suggested that, when vesicles were present, Ch nucleation times were an inverse function of Ch  $A_T$ ; the higher the Ch  $A_T$  in the system, the shorter the Ch nucleation time [18]. In the present study, similar techniques were employed to determine  $A_T$  of Ch and Ch nucleation times over wide ranges of CSI, BS to L molar ratios, and total lipid concentrations in supersaturated TC–L and TCDC–L solutions. Eighteen systems (see Tables 1–4) in which vesicles were present were chosen in this study. Data examination revealed that the results from these 18 systems conform well ( $R^2=0.972$ ) to the expression:

$$\text{Nucleation time (day)} = A' \times 10^{-B \cdot \text{Ch } A_T} \quad (2)$$

where  $A' = 1.56 \times 10^6$  day;  $B = 4.06$ .

When the scale of nucleation times is expressed logarithmically, the above equation can be rearranged as,

$$\text{Log (Nucleation Time)} = 6.193 - 4.06 \times \text{Ch } A_T \quad (3)$$

Based on Eq. (3) and the experimental measurements of the Ch nucleation times and the Ch  $A_T$ , the relationship between the logarithm of the Ch nucleation times and the Ch  $A_T$  values can be seen in Fig. 1 as a straight line. The number adjacent to each data point in Fig. 1 is the sample number from Tables 1–4. Consistent with the  $R^2$  value of 0.972, the experimental data are generally quite close to the

Table 1

Lipid particles present at the time of Ch  $A_T$  measurements and Ch nucleation times determined by QLS and microscopy in TCDC–L systems supersaturated with Ch

Phase region <sup>a</sup>	Sample number	Lipid composition (mM)			TCDC/L ratio	CSI	Ch $A_T$	Particles	Ch nucleation times
		TCDC	L	Ch					
I	1	44.0	22.0	9.65	2.0	1.82	1.08	Vesicles	79 days
I	2	72.9	21.2	10.56	3.4	1.82	1.36	Vesicles	3 days
I	3	72.9	21.2	11.35	3.4	1.95	1.39	Vesicles	3 days
I	4	111.9	22.0	12.22	5.1	1.94	1.67	Vesicles	6 h
I (near micellar zone)	5	72.9	21.2	7.66	3.4	1.32	1.12	Micelles only	>50 days
I	6	111.9	22.0	9.64	5.1	1.53	1.31	Micelles only	>9 days

<sup>a</sup> See text for definitions of I and II.

Table 2

Lipid particles present at the time of Ch  $A_T$  measurements and Ch nucleation times determined by QLS and microscopy in TC–L systems supersaturated with Ch

Phase region <sup>a</sup>	Sample number	Lipid composition (mM)			TC/L ratio	CSI	Ch $A_T$	Particles	Ch nucleation times
		TC	L	Ch					
I (near micellar zone)	7	72.9	21.2	6.19	3.4	1.32	1.15	Micelles only	>50 days
I	8	111.9	22.0	7.97	5.1	1.63	1.35	Micelles only	>50 days
II	9	44.0	22.0	8.85	2.0	2.01	1.16	Vesicles	37 days
II (near I)	10	55.0	20.0	7.01	2.8	1.56	1.20	Vesicles	23 days
I	11	72.9	21.2	9.70	3.4	2.06	1.32	Vesicles	6 days
I	12	80.0	20.0	10.13	4.0	2.15	1.37	Vesicles	6 days
I	13	72.9	21.2	12.00	3.4	2.55	1.41	Vesicles	4 days
I	14	111.9	22.0	12.54	5.1	2.56	1.67	Vesicles	6 h

<sup>a</sup> See text for definitions of I and II.

best straight line. It is noteworthy that Eq. (3) well represents the data over approximately a 1000-fold range of Ch nucleation times and that the experimental data are for both the TC–L and the TCDC–L systems. It is also noteworthy (see Tables 1–4) that wide ranges of BS–L ratios and total lipid concentrations were included in this study.

The influence of added calcium ions on both Ch  $A_T$  and Ch nucleation times are presented in Table 5 and Fig. 2. All four experiments of Table 5 yielded Ch  $A_T$  values and nucleation times that were in good agreement with Eq. (3). In Fig. 2, it is shown how the presence of  $\text{Ca}^{2+}$  changes both Ch  $A_T$  and the nucleation time; however, all of the data pairs remain close to the original correlation line.

### 3.2. Ch $A_T$ versus CSI concept

Although it has been recognized for some time that CSI may not be a good predictor of Ch supersaturation [4–9,18], it is worthwhile to consider the possible correlation (or the lack thereof) between CSI and Ch nucleation times with the present data. The data of the 18 systems are presented in Fig. 3 in a manner similar to that of Fig. 1, i.e., data plotted as the logarithm of Ch nucleation time versus CSI. As can be seen, the correlation is quite poor. From a statistical analysis, the  $R^2$  value is only 0.145 (compared to 0.972 in Fig. 1) if a linear relationship is assumed.

This poor correlation can be understood by an examination of Figs. 4 and 5 where plots of Ch  $A_T$  versus CSI are presented for the TC–L and the TCDC–L cases, respectively. First, it can be seen here that, for both the TC–L and

the TCDC–L cases, Ch  $A_T$  and CSI are essentially equal for unsaturated and saturated solutions, i.e., when  $\text{Ch } A_T \approx \text{CSI} \leq 1.0$ . However, for Ch-supersaturated solutions, CSI is no longer proportional to Ch  $A_T$  and no longer a single-valued function of Ch  $A_T$ ; this is equivalent to Henry's law not being obeyed for  $\text{Ch } A_T \geq 1.0$ . In physiological bile, the BS/L molar ratio is in the range from 2.5 to 3.5 [21], which is well represented in Figs. 4 and 5. From this result, it is not surprising that CSI is often found to be a poor measure of the Ch nucleation tendency in supersaturated biles.

### 3.3. Role of vesicles as nucleation catalysts

Evidence from the present study and that from an earlier study [18] strongly support vesicles being catalysts for Ch nucleation: Ch nucleation times are much shorter when vesicles are present. Table 1 shows that, for sample 6, this solution without vesicles was stable for more than 9 days even though the Ch  $A_T$  value (1.31) was nearly the same as sample 2, which nucleated in 3 days. Also, it is seen from Table 2 that sample 8 (Ch  $A_T \sim 1.35$ ), which did not contain vesicles was stable for more than 50 days, while sample 12 (Ch  $A_T \sim 1.37$ ) nucleated in 6 days.

Another aspect of interest here is the evidence from a previous study [27] that vesicles may represent only a small proportion ( $\sim 3\%$ ) of the total lipids, although they dominate scattered light because of their large sizes. In samples 1–3, the hydrodynamic radius of vesicles measured by QLS was  $\sim 200\text{--}500 \text{ \AA}$ , which is close to the size of vesicles formed in

Table 3

Lipid particles present at the time of Ch  $A_T$  measurements and Ch nucleation times determined by QLS and microscopy in supersaturated TC–L systems of the same TC/L molar ratio but different total lipid concentrations

Phase region <sup>a</sup>	Sample number	Lipid composition (mM)			TC/L ratio	CSI	Ch $A_T$	Total lipid (g/dl)	Particles	Ch nucleation times
		TC	L	Ch						
I or II	15	15	5	2.2	3.0	2.0	1.08	1.3	Vesicles	92 days
I or II	16	30	10	4.5	3.0	2.0	1.15	2.6	Vesicles	35 days
I or II	17	60	20	9.0	3.0	2.0	1.28	5.1	Vesicles	8 days
I or II	18	120	40	17.4	3.0	2.0	1.39	10.2	Vesicles	2 days

<sup>a</sup> See text for definitions of I and II.

Table 4

Lipid particles present at the time of Ch  $A_T$  measurements and Ch nucleation times determined by QLS and microscopy in supersaturated TC–L (samples 19 and 20) and TCDC–L (samples 21 and 22) systems

Phase region <sup>a</sup>	Sample number	Lipid composition (mM)			BS/L ratio	CSI	Ch $A_T$	Total lipid (g/dl)	Particles	$I_{sol}/I_{tol}$	Ch nucleation times
		BS	L	Ch							
II (but near I)	19	91.0	31.8	13.5	2.9	1.9	1.28	7.9	Vesicles	289	12 days
I	20	63.4	10.6	4.8	6.0	2.0	1.51	4.4	Vesicles	135	1 day
I	21	91.0	31.8	17.0	2.9	2.0	1.55	7.9	Vesicles	346	12 h
I	22	68.7	10.6	6.1	6.5	2.1	1.83	4.6	Vesicles	105	3 h

<sup>a</sup> See text for definitions of I and II.

80–32 mM tauroursodeoxycholate (TUDC)–L solutions with a Ch concentration of 6.5 mM [27]. Moreover, the total scattered light intensity of vesicles with respect to toluene ( $I_{sol}/I_{tol}$ ) in samples 1–3 was close to that of the 80–32 mM TUDC–L system (300–350). These findings indicate that it is likely that vesicles also represent a small proportion of the total lipid content in model bile solutions of different total lipid concentrations, as reported previously [27].

### 3.4. Influence of lipid concentrations and the question of vesicle aggregation in Ch nucleation

Previous studies [21,28,35,36] have shown that, when the BS to L molar ratio of bile is mainly between 2.5 and 3.5, Ch crystallites nucleate from concentrated gallbladder bile ( $\sim 10$  g/dl) of gallstone patients much more rapidly than from more dilute hepatic bile ( $\sim 3$  g/dl). A possible explanation for this observation has been provided by Halpern et al. [9,15] and Strasberg et al. [28,29]: when the

total lipid concentration increases, vesicles are in closer proximity; this promotes both vesicle aggregation and the onset of crystallite nucleation.

Another explanation can be gleaned from the data of Table 3. Here, it is seen that, at constant TC/L molar ratio (3:1) and constant CSI ( $\sim 2.0$ ), Ch  $A_T$  has increased significantly (from 1.08 to 1.39) with increasing total lipid concentration. This is accompanied by a decrease in Ch nucleation times from 92 to 2 days. Thus, it can be argued that the significant increase in Ch nucleation tendency with increasing total lipid concentration is only a result of increased Ch supersaturation (i.e., increased Ch  $A_T$ ).

While in the foregoing, it has been argued that Ch  $A_T$  (and the nucleation tendency) may increase with increasing total lipids, an opposite outcome can be seen in the results shown in Table 4. As seen in Table 4, the experiments with the higher total lipid concentrations yielded longer Ch nucleation times; but here again, the correlation between Ch nucleation times and Ch  $A_T$  values was quite good (Fig. 1).

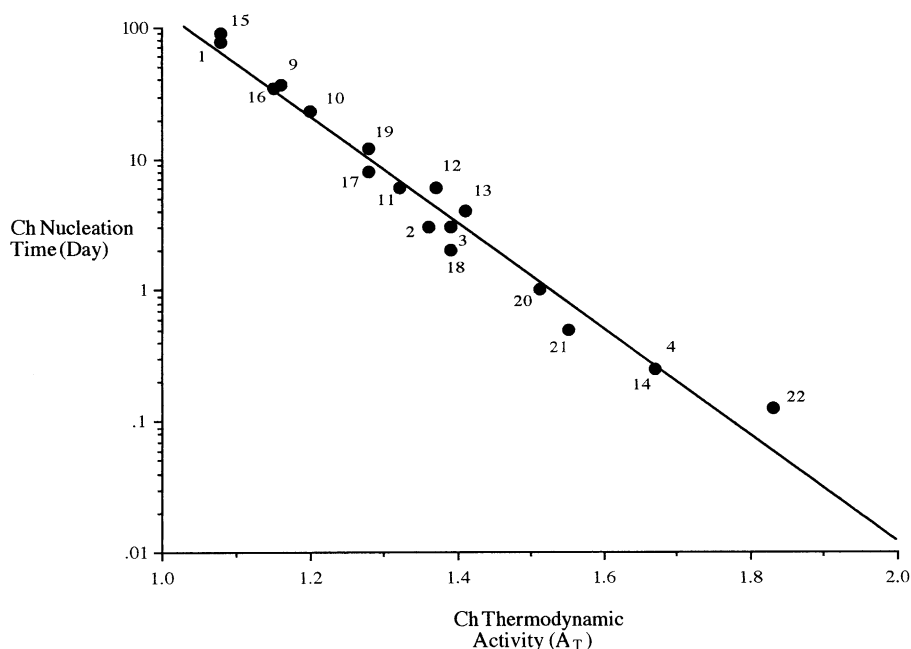


Fig. 1. Logarithm of Ch nucleation time (day) vs. Ch  $A_T$  when vesicles are present. Numbers adjacent to data points are sample numbers from Tables 1–4. Solid line indicates the best fit line.



Table 5

Lipid particles present at the time of Ch  $A_T$  measurements and Ch nucleation times determined by polarized microscope in supersaturated TC–L (sample 23) and TCDC–L (samples 24–26) systems

Sample number	Lipid composition (mM)			BS/L ratio	$\text{Ca}^{2+}$ (mM)	Ch $A_T$	Particles	Ch nucleation times
	BS	L	Ch					
23	72.9	21.2	9.7	3.4	10.0	1.63	Vesicles	9 h
24	72.9	21.2	11.4	3.4	10.0	1.76	Vesicles	3 h
25	44.0	22.0	9.6	2.0	5.0	1.35	Vesicles	3 days
26	44.0	22.0	9.2	2.0	5.0	1.29	Vesicles	6 days

### 3.5. Effect of calcium ions on Ch $A_T$ and Ch nucleation

Calcium has been considered among Ch nucleation pronucleating agents [29–34]. According to the vesicle aggregation/fusion hypothesis [37,38], it has been suggested that  $\text{Ca}^{2+}$  may help overcome the repulsion of the polar phospholipid head groups on the vesicles and thereby assist in promoting vesicle aggregation, vesicle fusion and Ch nucleation.

The results of the present study (Fig. 2) have clearly demonstrated a pronucleating effect of  $\text{Ca}^{2+}$  upon the Ch nucleation process. At 5 to 10 mM level of  $\text{Ca}^{2+}$ , the Ch nucleation times are reduced by a factor of 10 or more. It is quite interesting that the enhanced nucleation appears to be entirely associated with the increased thermodynamic activity of Ch; there is no evidence of  $\text{Ca}^{2+}$  influencing any “kinetic” factors involved. There is more discussion later on the  $\text{Ca}^{2+}$  effect.

### 3.6. A comparison of the present results with the work of Wang and Carey [39]

Wang and Carey, with the earlier work of Konikoff et al. [40] as a starting point, conducted a comprehensive study of crystallization pathways during Ch precipitation from model biles. These investigators observed the appearance of several Ch crystal forms and/or crystal habits in addition to the plate-like ChM crystals as functions of time and increasing lecithin concentration. The order of appearance of crystals, including ChM, varied depending upon the conditions of the supersaturated model bile solutions.

The basic aim and scope of our study have differed significantly from those of Wang and Carey and the results of their work were not available to us during the experimental phase of our study. Nonetheless, as there are important areas of overlap between the present work and that of Wang and Carey, a comparison of the results of the two studies should be of interest.

It is worthwhile to first point out that the aim of the present research, as was also our previous study [18], was to test the hypothesis that there should be a quantitative relationship between Ch nucleation time and Ch  $A_T$ . The Ch nucleation time was to be determined by both QLS and by microscopic observation. Ch  $A_T$  was to be determined at a time preceding the nucleation event so that no significant supersaturation relief would have occurred due to Ch precipitation [18]. Such data were to therefore provide unambiguous information for determining the relationship between Ch nucleation induction time and the driving force for Ch nucleation (i.e., Ch  $A_T$ ). The experiments of Wang and Carey generally differed from

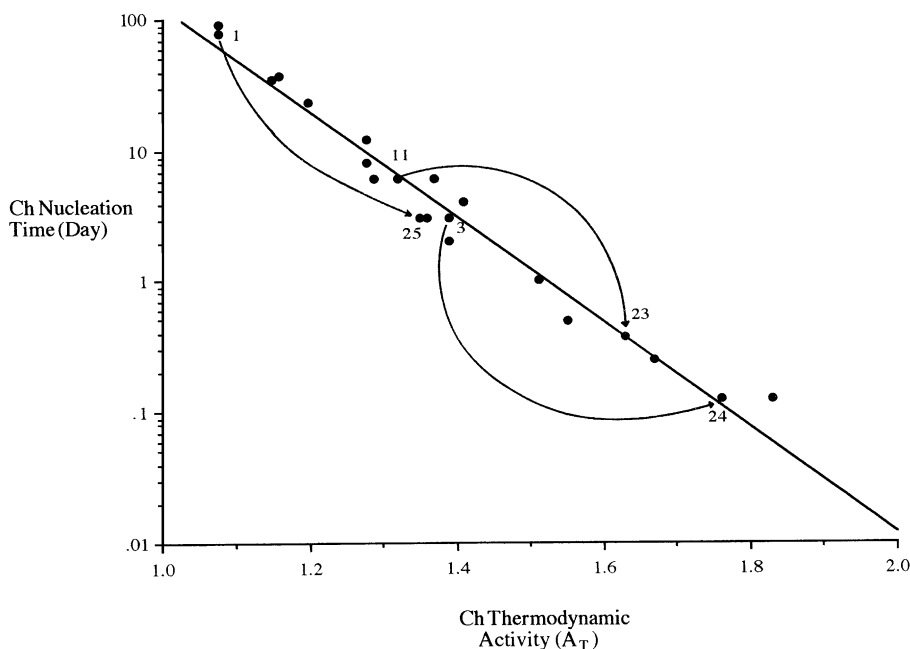


Fig. 2. Influence of  $\text{Ca}^{2+}$  on Ch  $A_T$  and Ch nucleation times when vesicles are present. Numbers adjacent to data points are sample numbers from Tables 1–5. Solid line indicates the best fit line from Fig. 1. Arrows indicate the movement of systems due to presence of  $\text{Ca}^{2+}$ .

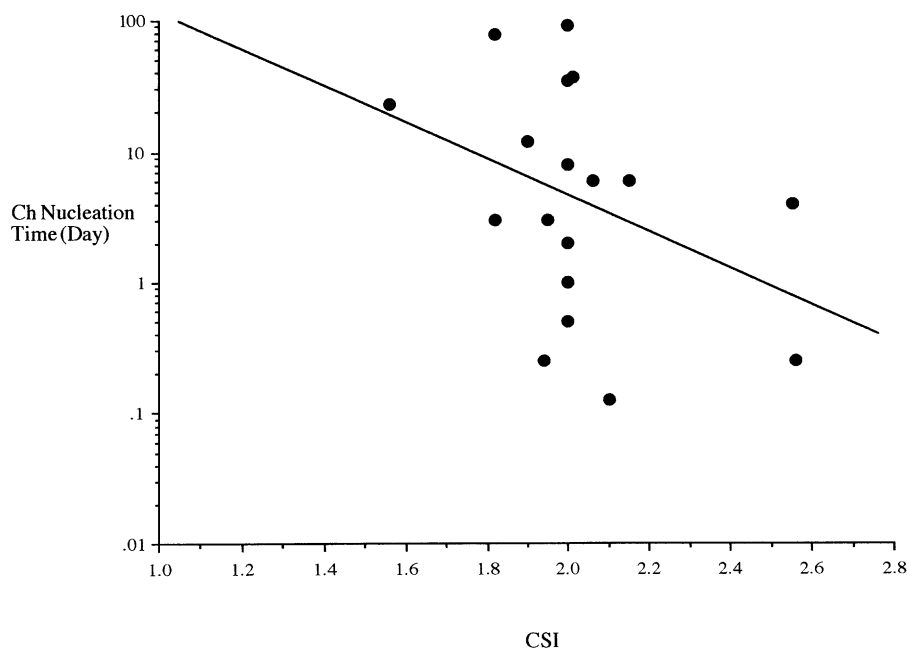


Fig. 3. Logarithm of Ch nucleation time (day) vs. CSI when vesicles are present. Systems are from Tables 1–4. Solid line indicates the best fit line.

ours in that their observations extended far into the crystallization/precipitation phase of the process, and Ch  $A_T$  would have been expected to decrease appreciably over the time period of the experiments. Another difference between our work and that of Wang and Carey is that the present work involves mainly Zone I of the equilibrium triangular phase diagram for the Ch–BS–L three component system, with a few experiments in or in the vicinity of Zone II (see Tables

1–4). Here, the zones are defined as follows. Zone I is the left two-phase zone of the phase diagram containing micelles and Ch crystals, Zone II is the central three-phase zone containing micelles, vesicles, and Ch crystals, and Zone III would be the right two-phase zone containing micelles and vesicles, but no crystals. The phase diagrams provided by Cabral and Small [41] were used to determine the appropriate zone for sample in Tables 1–4. We conducted no experiments in Zone

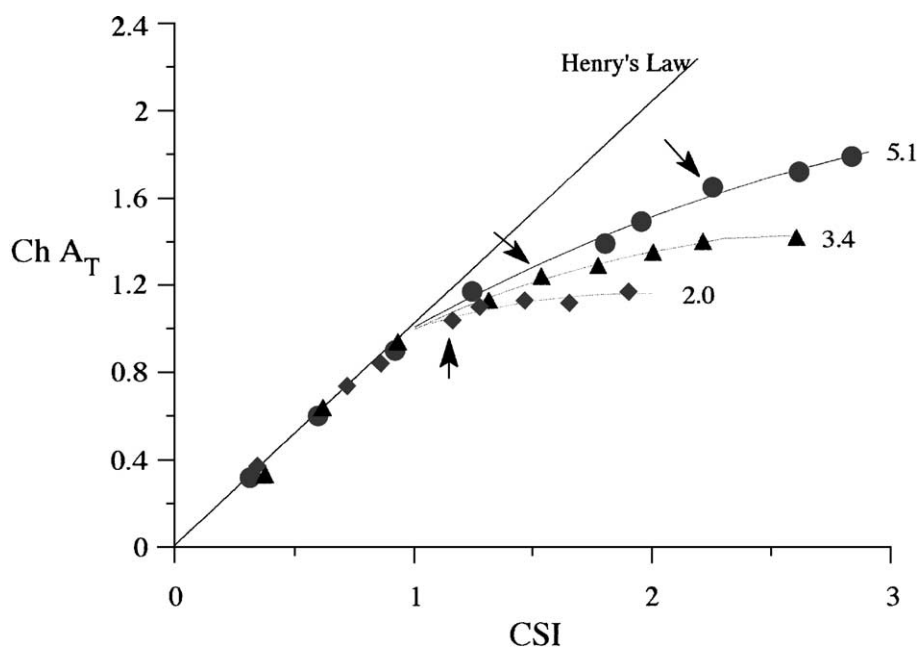


Fig. 4. The relationship between Ch  $A_T$  and CSI in TC–L system. (●) indicates TC–L = 111.9–22 mM, TC/L = 5.1; (▲) indicates TC–L = 72.9–21.2 mM, TC/L = 3.4; (◆) indicates TC–L = 44–22 mM, TC/L = 2.0. Arrows indicate visual turbidity at 4 h from silicone polymer uptake study.

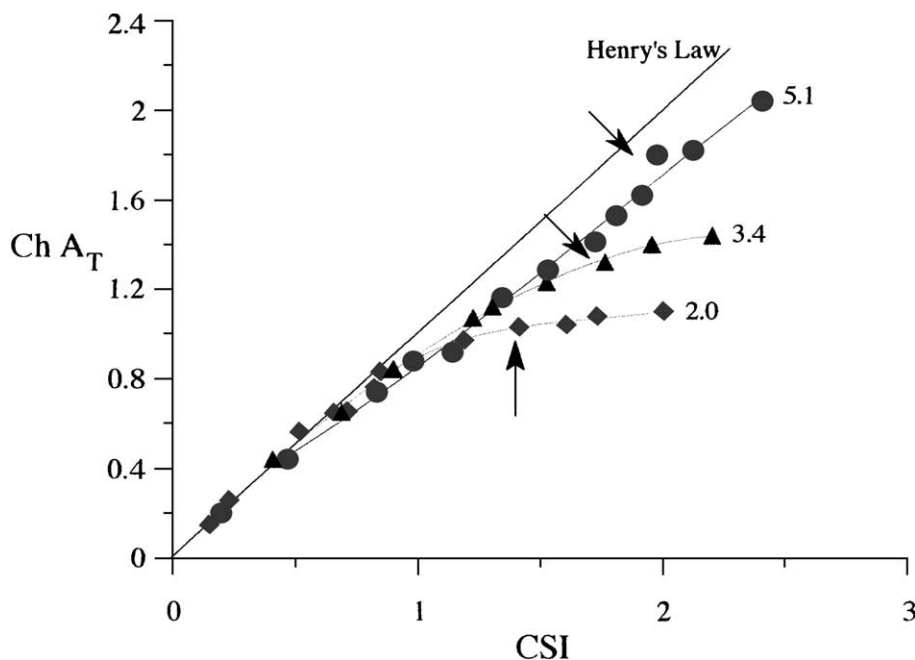


Fig. 5. The relationship between  $\text{Ch } A_T$  and CSI in TCDC-L system. (●) indicates TCDC-L = 111.9–22 mM, TCDC/L = 5.1; (▲) indicates TCDC-L = 72.9–21.2 mM, TCDC/L = 3.4; (◆) indicates TCDC-L = 44–22 mM, TCDC/L = 2.0. Arrows indicate visual turbidity at 4 h from silicone polymer uptake study.

III but Wang and Carey carried out representative studies in all three zones (I, II and III) of the equilibrium triangular phase diagrams.

### 3.6.1. Crystal detection time as a function of the BS/L ratio

An important result of the Wang and Carey study was the finding that the crystal detection time (same as our Ch nucleation time) increased with decreasing BS/L ratio over the entire range of their studies for both the TCDC-L-Ch and the TC-L-Ch systems. This finding is very consistent with the results of our present work. As a specific example, compare sample 3 and sample 4 of Table 1. Here the CSI values are essentially the same (1.95 and 1.94) while the TCDC/L ratios are 3.4 and 5.1 for sample 3 and sample 4, respectively. The nucleation times are 3 days for sample 3 and 6 h for sample 4. Another example: compare sample 13 and 14 of Table 2; again, the CSI values are essentially the same; the TC/L ratios are 3.4 and 5.1 while the nucleation times are 4 days and 6 h for samples 13 and 14, respectively. A generalization of these results can be found by considering Fig. 1 together with the results shown in Figs. 4 and 5 for the TC-L-Ch and the TCDC-L-Ch systems. In both Figs. 4 and 5, the L concentration was held relatively constant ( $\sim 22$  mM) while the BS concentration was varied. It can be clearly seen that as the BS/L ratio is increased,  $\text{Ch } A_T$  is increased in both systems. Thus, together with the plot of Fig. 1, one can see that the increase in Ch nucleation time with decreasing BS/L ratio may be correlated with the decrease in  $\text{Ch } A_T$ .

An important point that now deserves some discussion is that Wang and Carey determined crystal detection times for

both ChM and anhydrous cholesterol (ACh).<sup>1</sup> In our studies, no distinction was made; however, the needle-shaped or the conventional plate-like ChM crystals were observed in different instances as the earliest microscopic detection of crystals in our experiments. Significantly, as mentioned earlier, the nucleation times determined by QLS and those determined by microscopic observation generally agreed quite well in our studies [18]. In the Wang and Carey study, while crystal detection times increased with decreasing BS/L ratio for both ACh and ChM crystals, there was a cross-over in the data plots for the two crystal forms: for the high BS/L ratio region [ $\text{BS/L} \geq 7.0$ ], ACh appeared more rapidly (by around  $1.5 \times$ ) than ChM; for the low BS/L ratio region [ $\text{BS/L} \leq 7.0$ ], ChM appeared more rapidly (by  $\sim 2 \times$ ). It is noteworthy that in the Wang and Carey study the crystal detection times for ACh and ChM did not differ by more than about a factor of 2 over the entire range of study. Therefore, in the plot of Fig. 1, where the nucleation times are over about a 1000-fold range, the ACh and the ChM results could easily have fallen within the data scatter of both. Also, as discussed above (see also Figs. 4 and 5),  $\text{Ch } A_T$  would likely have been higher for model bile having higher BS/L ratios, it is possible this factor that may be the reason for the ACh crystals appearing earlier than the ChM

<sup>1</sup> Citing the work of Konikoff et al. [40], Wang and Carey offer a caveat that “the crystals were apparently ACh crystals as revealed by their habits, suggestive synchrotron X-ray spacings, and appropriate density. Nevertheless, more refined studies have yet to be carried out to conclusively prove that ACh and not a new ChM polymorph precipitates from bile under these circumstances.”



crystals at the high BS/L ratio in the Wang and Carey study. We have anecdotally noted in a few limited instances (see, for example, Figs. 2 and 3 in Ref. [18]) that, at high Ch  $A_T$ , needle-shaped crystals appeared before the plate-like crystals and, at low Ch  $A_T$ , only the plate-like Ch could be seen during the entire time period of the experiment. We may speculate at this point that the kinetics of nucleation may favor the appearance of ACh at high  $A_T$  while both kinetics and/or the thermodynamics may favor ChM at low  $A_T$  values. Future systematic studies should provide clarification of this issue.

### 3.6.2. Influence of calcium concentration

Wang and Carey reported that crystal detection times in the presence of added calcium ions were comparable to control biles without calcium; however, they systematically found that crystal numbers of both ACh and ChM increased with increased calcium concentration. Although it is unclear why crystal detection times did not correlate with increased crystal numbers, the latter suggests increased crystal nucleation rates with increased calcium concentration; this is in good agreement with our results (Fig. 2). The absence of a correlation between increased crystal numbers and the crystal detection times in the Wang and Carey study remains to be clarified.

### 3.7. Mechanistic and theoretical aspects of the present results

It should be instructive to first review from nucleation theory the viewpoint that the results presented in Fig. 1 are not consistent with homogeneous nucleation theory but are likely in agreement with heterogeneous nucleation (i.e., catalysis by vesicles). From classical homogeneous nucleation theory [42], one may write

$$\ln S^* = \left[ \frac{32\sigma^3 v^2}{3(kT)^3 \ln A} \right]^{\frac{1}{2}} \quad (4)$$

Here  $S^*$  is the critical supersaturation below which crystal nucleation is very slow and above which nucleation is very fast. The critical supersaturation is usually chosen to correspond to the rate of production of one nucleus per second per unit volume of supersaturated solution. The other parameters in Eq. (4) are  $v$  (molecular volume of Ch),  $\sigma$  (the Ch crystal solution interfacial tension),  $kT$  (the thermal energy), and  $A$  (the pre-exponential kinetic factor, which, for most purposes, is taken to equal  $\sim 10^{25} \text{ s}^{-1} \text{ cm}^{-3}$ ). From Ch precipitation experiments in 63% ethanol–water systems, Walton [42] deduced an  $S^*$  value of  $S^* \sim 15$  and a  $\sigma$  value of  $\sigma \sim 15 \text{ ergs/cm}^2$ . In their studies on Ch solubilization and precipitation in model bile solutions, Mazer and Carey [43] concluded that  $S^*$  for homogeneous Ch nucleation in Ch supersaturated in TC (simple micelles only) solution was probably  $S^* > 6.8$ , from which these investigators deduced  $\sigma$  for this system to be  $\sigma > 12.8 \text{ ergs/cm}^2$  based

on Eq. (4). Although the 6.8 value has involved some assumptions regarding Ch binding to simple TC micelles, these appear to be quite reasonable. Mazer and Carey point out the consistence of their result with Walton's result. Thus, it seems to be very likely Ch homogeneous nucleation conditions were being assessed in both instances. From this, it seems not unreasonable to believe that, for homogeneous nucleation of Ch in micellar bile salt only systems or in ethanol–water systems, a rather high  $S^*$  would be required (i.e.,  $S^* \geq 6.8$ ). It is evident that the modest supersaturation range (i.e., the Ch  $A_T$  range of 1.1 to 1.85) in Fig. 1 is far below the  $S^*$  values of Walton (for ethanol–water systems) and of Mazer and Carey (for TC only systems). The data of Fig. 1 would therefore not be consistent with homogeneous nucleation and may be best explained on the basis of heterogeneous nucleation, i.e., nucleation catalyzed by vesicles.

At this point, it is worthwhile to point out that the experimental nucleation time (crystal detection time in the Wang and Carey work) can be a function of both nucleation kinetics and crystal growth kinetics. When crystal growth rates are rapid, the nucleation time can be true measure of the inverse of the rate of nucleation. The exponential nature of the relationship between nucleation time and Ch  $A_T$  (see Eq. (2) and Fig. 1) would suggest a nucleation process and not simple diffusion-controlled crystal growth (which would be expected to follow a first-order dependence upon the concentration supersaturation, i.e., the differential between solution Ch concentration and Ch solubility). Significant contribution from a more complex crystal growth mechanism involving cooperativity of Ch molecules in the rate-determining step (e.g., two-dimensional nucleation controlled crystal growth), however, cannot be ruled out simply because of the exponential dependence. Perhaps the most persuasive evidence that crystal growth rates are likely not contributing significantly to Ch nucleation times comes from the fact that the QLS determined times for the “sudden” appearance of large particles ( $>700 \text{ \AA}$ ) are of the same magnitude as nucleation times observed microscopically (the microscopically determined nucleation times are only 1.2 to 1.4 times greater [18]). Also, microscopically observed crystals are typically in the micron size range. Therefore, it seems reasonable to assume relatively rapid growth of crystals relative to the Ch nucleation rate for the results presented in Fig. 1.

We now come to the important question of what is the nature of the mechanism of Ch nucleation catalysis by vesicles. Here it is helpful to use a scenario presented by MacDonald [44] as a starting point. As  $A_T \rightarrow 1.0$ , Ch molecules in a phospholipid bilayer will begin to associate laterally. The propensity for lateral association and for Ch phase separation should increase with increasing  $A_T$ . Possibly, with increasing  $A_T$ , Ch may tend to form a relatively rigid two-dimensional patch at the bilayer surface. MacDonald suggests at this point that, as true nucleation would require growth in the third dimension, flat Ch surfaces on adjacent

membranes may tend to adhere. Here,  $\text{Ca}^{2+}$  may assist to reduce the repulsive electrostatic effects in the adjacent regions of the bilayer. The highest probability of this process occurring would be in multilamellar liposomes or with aggregated vesicles as the interacting membrane surfaces have no chance of being far from each other. This scenario is plausible in light of, even at  $A_T \sim 1.0$ , the mole fraction of Ch in phospholipid bilayers can be as high as  $\sim 0.50$ . The catalytic effect of vesicles vis-a-vis the homogeneous nucleation barrier then likely arises from the favorable micro-environment provided by the bilayer(s) allowing the formation of an incipient crystal (i.e., the critical nucleus) with minimum free energy penalty. It would seem reasonable to speculate here that, perhaps, the presence of two membranes might not be necessary. This can arise if the free energy increment ingoing from the Ch monolayer patch (the embryo crystal in a single bilayer) to the Ch critical nucleus remains small; the need for the second membrane can then be circumvented. Unfortunately, both experimental and theoretical information is lacking on this issue.

The final point for discussion is that of the role of calcium in Ch nucleation. As mentioned earlier, it appears that the enhancement of Ch nucleation by calcium might be explained entirely on the basis of thermodynamics, i.e., on the basis that the presence of calcium simply moves the nucleation time downwards in the plot of Fig. 2, and three examples of this are shown. If one wishes to argue that it is *only* such a thermodynamic effect, one then must suggest that all kinetic factors must remain unchanged when calcium is added to the system. This would mean that the pre-exponential factor (not the same, but analogous to  $A$  in Eq. (4)) would remain unchanged. Here the pre-exponential factor is related to the local interfacial transport of Ch molecules. Additionally, it would require that calcium may not play a role assisting in overcoming the repulsion of polar phospholipid head groups at vesicle surfaces (and helping to promote vesicle aggregation, vesicle fusion and Ch nucleation). An alternate interpretation of the results of Fig. 2 would be that, while calcium increase  $A_T$  and the reduced Ch nucleation time does follow the straight line relationship obeyed by the 22 BS–L–Ch systems not containing calcium, this may be a coincidence arising from compensating cancellation of effects involving the above-mentioned kinetic factors.

#### 4. Conclusions

In the present investigation, a modified silicone polymer film uptake method has been used successfully to measure the true Ch supersaturation (Ch  $A_T$ ) in model biles over a wide range of conditions. An important finding of this research has been that the Ch nucleation time in supersaturated model biles is a single-valued function of the Ch  $A_T$  over a wide range of conditions. Another important finding has been that Ch–L vesicles are catalytic sites for Ch nucleation.

#### Acknowledgements

This work was supported by National Science Council (NSC-87-2312-B-259-001), Taiwan, ROC and the National Institute of Health (DK 32472), USA.

#### References

- [1] M.C. Carey, D.M. Small, The physical chemistry of cholesterol solubility in bile, *J. Clin. Invest.* 61 (1978) 998–1026.
- [2] M.C. Carey, Critical tables for calculating the cholesterol saturation of native bile, *J. Lipid Res.* 19 (1978) 945–955.
- [3] W.H. Admirand, D.M. Small, The physicochemical basis of cholesterol gallstone formation in man, *J. Clin. Invest.* 47 (1968) 1043–1052.
- [4] R.H. Dowling, G. Paumgartner, Summary discussion (Section III), *Hepatology* 12 (1990) 234S–244S.
- [5] S. Gallinger, P.R.C. Harvey, C.N. Petrunka, R.G. Ilson, S.M. Strasberg, Biliary proteins and the nucleation defect in cholesterol cholelithiasis, *Gastroenterology* 92 (1987) 867–875.
- [6] S. Gallinger, R.D. Taylor, P.R.C. Harvey, S.M. Strasberg, Effect of mucous glycoprotein on nucleation time of human bile, *Gastroenterology* 89 (1985) 648–658.
- [7] A.K. Groen, Nonmucous glycoproteins as pronucleating agents, *Hepatology* 12 (1990) 189S–194S.
- [8] K.R. Holan, R.T. Holzbach, R.E. Hermann, A.M. Cooperman, W.J. Claffey, Nucleation time: a key factor in the pathogenesis of cholesterol gallstone disease, *Gastroenterology* 77 (1979) 611–617.
- [9] Z. Halpern, M.A. Dudley, A. Kibe, M.P. Lynn, A.C. Breuer, R.T. Holzbach, Rapid vesicle formation and aggregation in abnormal human biles: a time-lapse video-enhanced contrast microscopy study, *Gastroenterology* 90 (1986) 875–885.
- [10] S.A. Ahrendt, K. Fox-Talbot, H.S. Kaufman, K.D. Lillemore, H.A. Pitt, Cholesterol nucleates rapidly from mixed micelles in the prairie dog, *Biochim. Biophys. Acta* 1211 (1994) 7–13.
- [11] D.L. Gantz, D.Q.H. Wang, M.C. Carey, D.M. Small, Cryoelectron microscopy of a nucleating model bile in vitreous ice: formation of primordial vesicles, *Biophys. J.* 76 (1999) 1436–1451.
- [12] S. Tao, S. Tazuma, G. Kajiyama, Fatty acid composition of lecithin is a key factor in bile metastability in supersaturated model bile systems, *Biochim. Biophys. Acta* 1167 (1993) 142–146.
- [13] P.H. Lee, D.C.H. Cheng, K. Takayama, W.I. Higuchi, Silicone polymer uptake method for determination of cholesterol thermodynamic activity in model bile systems, *J. Pharm. Sci.* 77 (1988) 610–614.
- [14] W.I. Higuchi, P.H. Lee, K. Takayama, U.K. Jain, N.A. Mazer, Cholesterol monomer activity and its role in understanding cholesterol saturation and crystallization, *Hepatology* 12 (1990) 88S–93S.
- [15] Z. Halpern, M.A. Dudley, M.P. Lynn, J.M. Nader, A.C. Breuer, R.T. Holzbach, Vesicle aggregation in model systems of supersaturated bile: relation to crystal nucleation lipid composition of the vesicular phase, *J. Lipid Res.* 27 (1986) 295–306.
- [16] A. Kibe, M.A. Dudley, Z. Halpern, M.P. Lynn, A.C. Breuer, R.T. Holzbach, Factors affecting cholesterol monohydrate crystal nucleation time in model systems of supersaturated bile, *J. Lipid Res.* 26 (1985) 1102–1111.
- [17] U.K. Jain, W.I. Higuchi, P.H. Lee, C.L. Liu, A rapid method for the measurement of cholesterol thermodynamic activity in bile salt–lecithin–cholesterol solutions, *J. Pharm. Sci.* 82 (1993) 714–720.
- [18] C.L. Liu, U.K. Jain, P.H. Lee, N.A. Mazer, W.I. Higuchi, Cholesterol thermodynamic activity, quasielastic light scattering and polarizing microscopy studies in aqueous taurocholate–lecithin solutions supersaturated with cholesterol, *J. Colloid Interface Sci.* 165 (1994) 411–424.
- [19] M.T. Subbiah, A. Kuksis, Alkaline solvent systems for thin-layer chromatography of bile acids, *J. Lipid Res.* 9 (1968) 288–290.

- [20] W.S. Singleton, M.S. Gray, M.L. Brown, J.L. White, Chromatographically homogeneous lecithin from egg phospholipids, *J. Am. Oil Chem. Soc.* 42 (1965) 53–56.
- [21] U.K. Jain, W.I. Higuchi, C.L. Liu, P.H. Lee, N.A. Mazer, Cholesterol (thermodynamic) activity determination in bile salt–lecithin–cholesterol systems and cholesterol-rich liquid crystalline mesophase formation, *Pharm. Res.* 9 (1992) 792–799.
- [22] C.L. Liu, Cholesterol binding to simple micelles in aqueous bile salt–cholesterol solutions, *J. Colloid Interface Sci.* 190 (1997) 261–268.
- [23] D.E. Cohen, M.R. Fisch, M.C. Carey, Principles of laser light-scattering spectroscopy: applications to the physicochemical study of model and native biles, *Hepatology* 12 (1990) 113S–122S.
- [24] N.A. Mazer, Quasielastic light scattering studies of aqueous biliary lipid systems and native bile, *Hepatology* 12 (1990) 39S–44S.
- [25] D.E. Koppel, Analysis of macromolecular polydispersity in intensity correlation spectroscopy: the method of cumulants, *J. Chem. Phys.* 57 (1972) 4814–4820.
- [26] P. Schurtenberger, N. Mazer, W. Kanzig, Micelle to vesicle transition in aqueous solutions of bile salt and lecithin, *J. Phys. Chem.* 89 (1985) 1042–1049.
- [27] C.L. Liu, U.K. Jain, W.I. Higuchi, N.A. Mazer, Quasielastic light scattering and cholesterol thermodynamic activity studies of the micelle-to-vesicle transition in conjugated ursodeoxycholate–lecithin–cholesterol solutions, *J. Colloid Interface Sci.* 162 (1994) 437–453.
- [28] S.M. Strasberg, J.L. Toth, S. Gallinger, P.R.C. Harvey, High protein and total lipid concentration are associated with reduced metastability of bile in an early stage of cholesterol gallstone formation, *Gastroenterology* 98 (1990) 1–8.
- [29] S.M. Strasberg, P.R.C. Harvey, Biliary cholesterol transport and precipitation: introduction and overview of conference, *Hepatology* 12 (1990) 1S–5S.
- [30] P.R.C. Harvey, G.A. Upadhyay, S.M. Strasberg, Immunoglobulins as nucleating proteins in the gallbladder bile of patients with cholesterol gallstones, *J. Biol. Chem.* 266 (1991) 13996–14003.
- [31] L.J. Lis, W.T. Lis, V.A. Parsegian, R.P. Rand, Adsorption of divalent cations to a variety of phosphatidylcholine bilayers, *Biochemistry* 20 (1981) 1771–1777.
- [32] P.F. Levy, B.F. Smith, J.T. LaMont, Human gallbladder mucin accelerates nucleation of cholesterol in artificial bile, *Gastroenterology* 87 (1984) 270–275.
- [33] A. Kibe, R.T. Holzbach, N.F. LaRusso, S.J.T. Mao, Inhibition of cholesterol crystal formation by apolipoproteins in supersaturated model bile, *Science* 225 (1984) 514–516.
- [34] T. Ohya, J. Schwarzendrube, N. Busch, S. Gresky, K. Chandler, A. Takabayashi, H. Igimi, K. Egami, R.T. Holzbach, Isolation of a human biliary glycoprotein inhibitor of cholesterol crystallization, *Gastroenterology* 104 (1993) 527–538.
- [35] P.R.C. Harvey, G. Somjen, M.S. Lichtenberg, C. Petrunka, T. Gilat, S.M. Strasberg, Nucleation of cholesterol from vesicles isolated from bile of patients with and without cholesterol gallstones, *Biochim. Biophys. Acta* 921 (1987) 198–204.
- [36] S.H. Gollish, M.J. Burnstein, R.G. Ilson, C.N. Petrunka, S.M. Strasberg, Nucleation of cholesterol monohydrate crystals from hepatic and gallbladder bile of patients with cholesterol gallstones, *Gut* 24 (1983) 836–844.
- [37] A.K. Groen, R. Ottenhoff, P.L.M. Jansen, J. van Marle, G.N.J. Tytgat, Effect of cholesterol nucleation-promoting activity on cholesterol solubilization in model bile, *J. Lipid Res.* 30 (1989) 51–58.
- [38] N. Duzgunes, Molecular control of vesicle aggregation and membrane fusion: hypotheses on bile vesicles, *Hepatology* 12 (1990) 67S–74S.
- [39] D.Q. Wang, M.C. Carey, Complete mapping of crystallization pathways during cholesterol precipitation from model bile: influence of physical–chemical variables of pathophysiologic relevance and identification of a stable liquid crystalline state in cold, dilute and hydrophilic bile salt-containing systems, *J. Lipid Res.* 37 (1996) 606–630.
- [40] F.M. Konikoff, D.S. Chung, J.M. Donovan, D.M. Small, M.C. Carey, Filamentous, helical, and tubular microstructures during cholesterol crystallization from bile: evidence that cholesterol does not nucleate classic monohydrate plates, *J. Clin. Invest.* 90 (1992) 1155–1160.
- [41] D.J. Cabral, D.M. Small, Physical chemistry of bile, in: S.G. Schultz, et al. (Eds.), *Handbook of Physiology, The Gastrointestinal System III*, Section 6, American Physiological Society, Waverly Press, Baltimore, MD, 1989, pp. 621–662, Chapter 31.
- [42] A.G. Walton, *The Formation and Properties of Precipitates*, Interscience, New York, 1967.
- [43] N.A. Mazer, M.C. Carey, Quasi-elastic light-scattering studies of aqueous biliary lipid systems: cholesterol solubilization and precipitation in model bile solutions, *Biochemistry* 22 (1983) 426–442.
- [44] R.C. MacDonald, Surface chemistry of phospholipid vesicles relevant to their aggregation and fusion, *Hepatology* 12 (1990) 56S–60S.